IEEE Access
Multidisciplinary | Rapid Review | Open Access Journal

SPECIAL SECTION ON ARTIFICIAL INTELLIGENCE FOR PHYSICAL-LAYER WIRELESS COMMUNICATIONS

Received September 28, 2019, accepted October 15, 2019, date of publication October 21, 2019, date of current version October 31, 2019.

Digital Object Identifier 10.1109/ACCESS.2019.2948475

GWO-BP Neural Network Based OP Performance Prediction for Mobile Multiuser Communication Networks

LINGWEI XU[1,2], (Member, IEEE), HAN WANG[3], (Member, IEEE), WEN LIN[2], (Member, IEEE), THOMAS AARON GULLIVER[4], (Senior Member, IEEE), AND KHOA N. LE[5], (Senior Member, IEEE)

[1]College of Information Science and Technology, Qingdao University of Science and Technology, Qingdao 266061, China
[2]Electronic Information and Control of Fujian University Engineering Research Center, Minjiang University, Fuzhou 350121, China
[3]College of Physical Science and Engineering, Yichun University, Yichun 336000, China
[4]Department of Electrical and Computer Engineering, University of Victoria, Victoria, BC V8W 2Y2, Canada
[5]School of Computing, Engineering and Mathematics, Western Sydney University, Kingswood, Sydney, NSW 2747, Australia

Corresponding authors: Lingwei Xu (gaomilaojia2009@163.com) and Han Wang (hanwang1214@126.com)

This work was supported in part by the National Natural Science Foundation of China under Grant U1806201, Grant 61671261, Grant 61901409, and Grant 61901207, in part by the Opening Foundation of Electronic Information and Control of Fujian University Engineering Research Center, Minjiang University under Grant MJXY-KF-EIC1801, in part by the Shandong Province Colleges and Universities Young Talents Initiation Program under Grant 2019KJN047, in part by the Opening Foundation of Key Laboratory of Opto-Technology and Intelligent Control (Lanzhou Jiaotong University), Ministry of Education under Grant KFKT2018-2, in part by the Shandong Province Postdoctoral Innovation Project under Grant 201703032, in part by the Shandong Province Natural Science Foundation under Grant ZR2017BF023, and in part by the Doctoral Foundation of QUST under Grant 010029029.

ABSTRACT The complexity and variability of wireless channels makes reliable mobile multiuser communications challenging. As a consequence, research on mobile multiuser communication networks has increased significantly in recent years. The outage probability (OP) is commonly employed to evaluate the performance of these networks. In this paper, exact closed-form OP expressions are derived and an OP prediction algorithm is presented. Monte-Carlo simulation is used to evaluate the OP performance and verify the analysis. Then, a grey wolf optimization back-propagation (GWO-BP) neural network based OP performance prediction algorithm is proposed. Theoretical results are used to generate training data. We also examine the extreme learning machine (ELM), locally weighted linear regression (LWLR), support vector machine (SVM), BP neural network, and wavelet neural network methods. Compared to the wavelet neural network, LWLR, SVM, BP, and ELM methods, the results obtained show that the GWO-BP method provides the best OP performance prediction.

INDEX TERMS Mobile multiuser communication, outage probability, performance prediction, GWO-BP neural network.

I. INTRODUCTION

The explosive growth in the number of mobile users has motivated research on fifth generation (5G) mobile communication systems [1]–[5]. Non-orthogonal multiple access (NOMA) has been proposed for 5G systems [6], and in [7] an effective deep learning scheme for NOMA systems was presented.

Cooperative communications is widely used in 5G mobile multiuser communication systems [8]–[11]. The outage performance of a multiuser relay system with amplify-and-forward (AF) relaying was investigated in [12]. A new precoder design was proposed in [13] for a multiuser AF relaying system. In [14], secure multiuser communications in a relaying system was examined. The secrecy performance of mobile cooperative networks over 2-Rayleigh fading channels was analysed in [15], [16]. Mobile cooperative communications over N-Rayleigh fading channels was examined in [17].

Only Rayleigh and Nakagami-m fading channels were considered in [8]–[17]. However, these channel models may not be suitable to characterize the complexities of practical mobile communication systems. The N-Nakagami model was considered in [18]–[20] for mobile communications.

The associate editor coordinating the review of this manuscript and approving it for publication was Guan Gui.

The outage probability (OP) can be used to characterize the performance of mobile multiuser communication systems over N-Nakagami fading channels. If the OP is poor, communications will be unreliable. Thus, it is important to predict the OP performance of these systems in complex and variable environments such as N-Nakagami fading channels. Because of the good nonlinear prediction capabilities, back-propagation (BP) neural networks have been widely used [21]. A novel bee colony algorithm was used to optimize a BP neural network in [22]. A BP-based detection algorithm was proposed for unmanned aerial vehicle systems in [23].

To date, OP performance prediction of mobile multiuser communication systems has not been considered. Therefore, this prediction is investigated here. The main contributions of this paper are as follows.

1. The OP performance of mobile multiuser communication networks is investigated considering transmit antenna selection (TAS). Exact closed-form expressions for the OP are derived which differ from those in [8]–[17].

2. OP performance prediction is analysed using the OP expressions obtained. A grey wolf optimization back-propagation (GWO-BP) neural network based OP performance prediction algorithm is presented. Theoretical OP results are used to generate training data. Simulation is used to evaluate the extreme learning machine (ELM), locally weighted linear regression (LWLR), support vector machine (SVM), wavelet neural network, GWO-BP neural network, and BP neural network methods. These results show that compared to the LWLR, SVM, BP, wavelet neural network, and ELM methods, the GWO-BP method provides the best OP performance prediction results.

3. The analysis is validated via Monte-Carlo simulation. The impact of fading and the system parameters on the OP performance are examined.

The remainder of this paper is organized as follows. The system model is given in Section II. The OP performance for two TAS schemes is derived in Sections III and IV, respectively. OP performance prediction using the GWO-BP method is presented in V. Section VI provides the simulation results, and finally Section VII gives some concluding remarks.

II. SYSTEM MODEL

Fig. 1 shows the system model. There is a mobile source (MS), L mobile users (MU), and a mobile relay (MR). The MS uses N_{t} antennas. G_{SR}=1, which is the relative gain of the MS→MR. The total power is E. h=h_k, and k∈{SUil, SRi, RUl}. h follows an N-Nakagami distribution [18].

In the first time slot, MS$_i$ transmits the x which has zero mean and variance 1. MU$_l$ and MR receive the signals as

$$r_{\mathrm{SU}il} = \sqrt{G_{\mathrm{SU}il}KE}h_{\mathrm{SU}il}x + n_{\mathrm{SU}il} \tag{1}$$

$$r_{\mathrm{SR}i} = \sqrt{KE}h_{\mathrm{SR}i}x + n_{\mathrm{SR}i} \tag{2}$$

where $G_{\mathrm{SU}il}$ is the relative gain of MS$_i$→MU$_l$, and $n_{\mathrm{SR}i}$ and $n_{\mathrm{SU}il}$ have means of 0 and variances of $N_0/2$. K is the power allocation parameter.

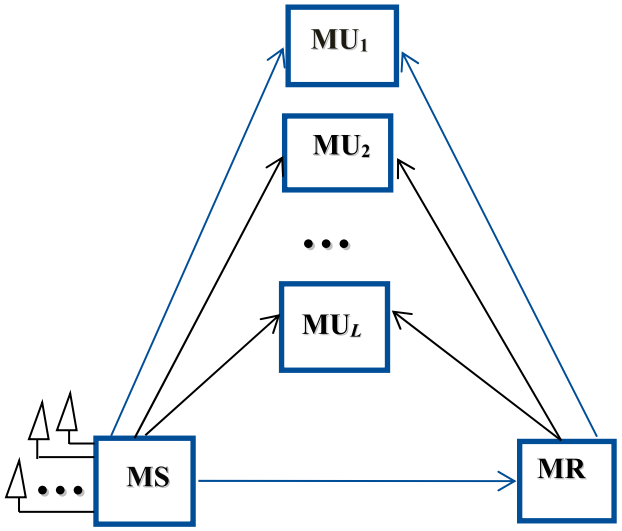

FIGURE 1. System model.

In the second time slot, the MR uses the decode and forward (DF) scheme so that MU$_l$ receives the signal as

$$r_{\mathrm{RU}l} = g\sqrt{G_{\mathrm{RU}l}(1-K)E}h_{\mathrm{RU}l}x + n_{\mathrm{RU}l} \tag{3}$$

$I_{\mathrm{SR}i}$ is the mutual information between MS$_i$ and the MR, which can be expressed as

$$I_{\mathrm{SR}i} = \frac{1}{2}\log_2(1+\gamma_{\mathrm{SR}i}) \tag{4}$$

where

$$\gamma_{\mathrm{SR}i} = \frac{K\left|h_{\mathrm{SR}i}\right|^2 E}{N_0} = K\left|h_{\mathrm{SR}i}\right|^2\overline{\gamma} \tag{5}$$

Let R is the spectral efficiency. If $I_{\mathrm{SR}i} < R$, the MR will not participate in the cooperation, namely,

$$\Pr(I_{\mathrm{SR}i} \le R) = \Pr(\frac{1}{2}\log_2(1+\gamma_{\mathrm{SR}i}) \le R) = \Pr(\gamma_{\mathrm{SR}i} \le \gamma_{\mathrm{th}}) \tag{6}$$

where

$$\gamma_{\mathrm{th}} = 2^{2R} - 1 \tag{7}$$

The signal-to-noise ratio (SNR) at MU$_l$ can be expressed as

$$\gamma_{il} = \begin{cases} \gamma_{\mathrm{SU}il}, & \gamma_{\mathrm{SR}i} \le \gamma_{\mathrm{th}} \\ \max(\gamma_{\mathrm{SU}il}, \gamma_{\mathrm{RU}il}), & \gamma_{\mathrm{SR}i} > \gamma_{\mathrm{th}} \end{cases} \tag{8}$$

where

$$\gamma_{\mathrm{SU}il} = \frac{KG_{\mathrm{SU}il}\left|h_{\mathrm{SU}il}\right|^2 E}{N_0} = KG_{\mathrm{SU}il}\left|h_{\mathrm{SU}il}\right|^2\overline{\gamma} \tag{9}$$

$$\gamma_{\mathrm{RU}il} = \frac{(1-K)G_{\mathrm{RU}il}\left|h_{\mathrm{RU}il}\right|^2 E}{N_0} = (1-K)G_{\mathrm{RU}il}\left|h_{\mathrm{RU}il}\right|^2\overline{\gamma} \tag{10}$$

The best user given by

$$\gamma_{\mathrm{SC}_i} = \max_{1\le l\le L}(\gamma_{il}) \tag{11}$$

is selected. For TAS scheme I, this is

$$\begin{aligned} \nu &= \arg \max_{1\le i\le N_{\mathrm{t}}} (\gamma_{\mathrm{SC}i}) \\ &= \arg \begin{cases} \max\limits_{1\le i\le N_{\mathrm{t}}, 1\le l\le L} (\gamma_{\mathrm{SU}il}), & \text{if } |C| = 0 \\ \max\limits_{j\in C, 1\le l\le L} (\gamma_{\mathrm{SU}l}, \gamma_{\mathrm{RU}jl}), & \text{if } |C| \neq 0 \end{cases} \end{aligned} \tag{12}$$

where the decoding set C is given as

$$C = \left\{ 1 \le j \le N_{\mathrm{t}} | \gamma_{\mathrm{SR}j} > \gamma_{\mathrm{th}} \right\} \tag{13}$$

$$\gamma_{\mathrm{SU}l} = \max_{1\le i\le N_{\mathrm{t}}} (\gamma_{\mathrm{SU}il}) \tag{14}$$

and $|C|$ is the cardinality of C.

For TAS scheme II, we select

$$k = \arg \max_{1\le i\le N_{\mathrm{t}}, 1\le l\le L} (\gamma_{\mathrm{SU}il}) \tag{15}$$

III. THE OP OF TAS SCHEME I

We obtain the OP as

$$\begin{aligned} &F_{\mathrm{optimal}}(R_{\mathrm{th}}) \\ &= \Pr(\gamma_{\mathrm{SC}} < R_{\mathrm{th}}) \\ &= \Pr(|C| = 0)\Pr(\max_{1\le i\le N_{\mathrm{t}}, 1\le l\le L} (\gamma_{\mathrm{SU}il}) < R_{\mathrm{th}}) \\ &\quad + \Pr(|C| \neq 0)\Pr(\max_{i\in C, 1\le l\le L} (\gamma_{\mathrm{SU}il}, \gamma_{\mathrm{RU}l}) < R_{\mathrm{th}}) \\ &= \Pr(|C| = 0)\Pr(\max_{1\le i\le N_{\mathrm{t}}, 1\le l\le L} (\gamma_{\mathrm{SU}il}) < R_{\mathrm{th}}) \\ &\quad + \sum_{n=1}^{N_{\mathrm{t}}} \binom{N_{\mathrm{t}}}{n} \Pr(|C| = n) \\ &\quad \times \Pr(\max_{1\le j\le n, 1\le l\le L} (\gamma_{\mathrm{SU}l}, \gamma_{\mathrm{RU}jl}) < R_{\mathrm{th}}) \\ &= \Pr(|C| = 0)V_1 + \sum_{n=1}^{N_{\mathrm{t}}} \binom{N_{\mathrm{t}}}{n} \Pr(|C| = n)V_2 \end{aligned} \tag{16}$$

where R_{th} is a given threshold, m is the fading coefficient, and

$$\Pr(|C| = 0) = \left(\frac{1}{\prod_{j=1}^{N} \Gamma(m_j)} G_{1,N+1}^{N,1} \left[\frac{\gamma_{\mathrm{th}}}{\overline{\gamma_{\mathrm{SR}}}} \prod_{j=1}^{N} \frac{m_j}{\Omega_j} \Big|_{m_1,\ldots,m_N,0}^{1} \right] \right)^{N_{\mathrm{t}}} \tag{17}$$

$$\begin{aligned} \Pr(|C| = n) &= \left(\frac{1}{\prod_{j=1}^{N} \Gamma(m_j)} G_{1,N+1}^{N,1} \left[\frac{\gamma_{\mathrm{th}}}{\overline{\gamma_{\mathrm{SR}}}} \prod_{j=1}^{N} \frac{m_j}{\Omega_j} \Big|_{m_1,\ldots,m_N,0}^{1} \right] \right)^{N_{\mathrm{t}}-n} \\ &\quad \times \left(1 - \frac{1}{\prod_{j=1}^{N} \Gamma(m_j)} G_{1,N+1}^{N,1} \left[\frac{\gamma_{\mathrm{th}}}{\overline{\gamma_{\mathrm{SR}}}} \prod_{j=1}^{N} \frac{m_j}{\Omega_j} \Big|_{m_1,\ldots,m_N,0}^{1} \right] \right)^{n} \end{aligned} \tag{18}$$

V_1 is given as

$$\begin{aligned} V_1 &= \Pr(\max_{1\le i\le N_{\mathrm{t}}, 1\le l\le L} (\gamma_{\mathrm{SU}il}) < R_{\mathrm{th}}) \\ &= \left(\frac{1}{\prod_{d=1}^{N} \Gamma(m_d)} G_{1,N+1}^{N,1} \left[\frac{R_{\mathrm{th}}}{\overline{\gamma_{\mathrm{SU}}}} \prod_{d=1}^{N} \frac{m_d}{\Omega_d} \Big|_{m_1,\ldots,m_N,0}^{1} \right] \right)^{N_{\mathrm{t}}\times L} \end{aligned} \tag{19}$$

$$\overline{\gamma_{\mathrm{SU}}} = KG_{\mathrm{SU}}\overline{\gamma} \tag{20}$$

V_2 is given as

$$\begin{aligned} V_2 &= \Pr(\max_{1\le j\le n, 1\le l\le L} (\gamma_{\mathrm{SU}l}, \gamma_{\mathrm{RU}jl}) < R_{\mathrm{th}}) \\ &= \Pr(\max_{1\le i\le N_{\mathrm{t}}, 1\le l\le L} (\gamma_{\mathrm{SU}il}) < R_{\mathrm{th}})\Pr(\max_{1\le j\le n, 1\le l\le L} (\gamma_{\mathrm{RU}jl}) < R_{\mathrm{th}}) \\ &= \left(\frac{1}{\prod_{d=1}^{N} \Gamma(m_d)} G_{1,N+1}^{N,1} \left[\frac{R_{\mathrm{th}}}{\overline{\gamma_{\mathrm{SU}}}} \prod_{d=1}^{N} \frac{m_d}{\Omega_d} \Big|_{m_1,\ldots,m_N,0}^{1} \right] \right)^{N_{\mathrm{t}}\times L} \\ &\quad \times \left(\frac{1}{\prod_{jj=1}^{N} \Gamma(m_{jj})} G_{1,N+1}^{N,1} \left[\frac{R_{\mathrm{th}}}{\overline{\gamma_{\mathrm{RU}}}} \prod_{jj=1}^{N} \frac{m_{jj}}{\Omega_{jj}} \Big|_{m_1,\ldots,m_N,0}^{1} \right] \right)^{n\times L} \end{aligned} \tag{21}$$

$$\overline{\gamma_{\mathrm{RU}}} = (1 - K)G_{\mathrm{RU}}\overline{\gamma} \tag{22}$$

IV. THE OP OF TAS SCHEME II

The SNR at the MU is

$$\gamma_{\mathrm{SC}} = \max(\gamma_{\mathrm{SU}k}, \gamma_{\mathrm{SRU}k}) \tag{23}$$

and the cumulative density function (CDF) of $\gamma_{\mathrm{SU}k}$ is

$$\begin{aligned} &F_{\gamma_{\mathrm{SU}k}}(r) \\ &= \Pr(\max_{1\le i\le N_{\mathrm{t}}, 1\le l\le L} (\gamma_{\mathrm{SU}il}) < r) \\ &= \left(\frac{1}{\prod_{d=1}^{N} \Gamma(m_d)} G_{1,N+1}^{N,1} \left[\frac{r}{\overline{\gamma_{\mathrm{SU}}}} \prod_{d=1}^{N} \frac{m_d}{\Omega_d} \Big|_{m_1,\ldots,m_N,0}^{1} \right] \right)^{N_{\mathrm{t}}\times L} \end{aligned} \tag{24}$$

The CDF of $\gamma_{\mathrm{SRU}k}$ is given as

$$\begin{aligned} &F_{\gamma_{\mathrm{SRU}k}}(r) \\ &= \Pr(\gamma_{\mathrm{SR}k} < \gamma_{\mathrm{th}}) + (1 - \Pr(\gamma_{\mathrm{SR}k} < \gamma_{\mathrm{th}}))F_{\gamma_{\mathrm{RU}k}}(r) \end{aligned}$$

$$= \left(\begin{array}{l} \frac{1}{\prod_{j=1}^{N} \Gamma(m_j)} G_{1,N+1}^{N,1} \left[\frac{\gamma_{\text{th}}}{\gamma_{\text{SR}}} \prod_{j=1}^{N} \frac{m_j}{\Omega_j} \Big|_{m_1,\ldots,m_N,0}^{1} \right] + \\ \left(1 - \frac{1}{\prod_{j=1}^{N} \Gamma(m_j)} G_{1,N+1}^{N,1} \left[\frac{\gamma_{\text{th}}}{\gamma_{\text{SR}}} \prod_{j=1}^{N} \frac{m_j}{\Omega_j} \Big|_{m_1,\ldots,m_N,0}^{1} \right] \right) \\ \times \frac{1}{\prod_{jj=1}^{N} \Gamma(m_{jj})} G_{1,N+1}^{N,1} \left[\frac{r}{\gamma_{\text{RU}}} \prod_{jj=1}^{N} \frac{m_{jj}}{\Omega_{jj}} \Big|_{m_1,\ldots,m_N,0}^{1} \right] \end{array} \right) \tag{25}$$

The OP is then

$$F_{\text{suboptimal}} = \left(\frac{1}{\prod_{d=1}^{N} \Gamma(m_d)} G_{1,N+1}^{N,1} \left[\frac{R_{\text{th}}}{\gamma_{\text{SU}}} \prod_{d=1}^{N} \frac{m_d}{\Omega_d} \Big|_{m_1,\ldots,m_N,0}^{1} \right] \right)^{N_t \times L} \times \left(\begin{array}{l} \frac{1}{\prod_{j=1}^{N} \Gamma(m_j)} G_{1,N+1}^{N,1} \left[\frac{\gamma_{\text{th}}}{\gamma_{\text{SR}}} \prod_{j=1}^{N} \frac{m_j}{\Omega_j} \Big|_{m_1,\ldots,m_N,0}^{1} \right] + \\ \left(1 - \frac{1}{\prod_{j=1}^{N} \Gamma(m_j)} G_{1,N+1}^{N,1} \left[\frac{\gamma_{\text{th}}}{\gamma_{\text{SR}}} \prod_{j=1}^{N} \frac{m_j}{\Omega_j} \Big|_{m_1,\ldots,m_N,0}^{1} \right] \right) \\ \times \frac{1}{\prod_{jj=1}^{N} \Gamma(m_{jj})} G_{1,N+1}^{N,1} \left[\frac{R_{\text{th}}}{\gamma_{\text{RU}}} \prod_{jj=1}^{N} \frac{m_{jj}}{\Omega_{jj}} \Big|_{m_1,\ldots,m_N,0}^{1} \right] \end{array} \right) \tag{26}$$

V. OP PERFORMANCE PREDICTION BASED ON THE GWO-BP NEURAL NETWORK

A. GWO ALGORITHM

In the GWO algorithm there are alpha (α), beta (β), delta (δ) and omega (ω) wolves [24].

The GWO algorithm is as follows.

1) PREY ENCIRCLING

The encircling behaviour of the GWO is calculated as follows:

$$\vec{D} = \left| \vec{C} \cdot \vec{X}_p(t) - \vec{X}(t) \right| \tag{27}$$

$$\vec{X}(t+1) = \vec{X}_p(t) - \vec{A} \cdot \vec{D} \tag{28}$$

where the coefficient vectors are $\vec{A}$ and $\vec{C}$, the distance between the prey and wolves is $\vec{D}$, the prey's position vector is $\vec{X}_p$, and $\vec{X}$ represents the wolves' position vector.

$\vec{A}$ and $\vec{C}$ are given as

$$\vec{A} = 2a \cdot \vec{r_1} - \vec{r_2} \tag{29}$$

$$\vec{C} = 2 \cdot \vec{r_2} \tag{30}$$

where $\vec{r_1}$, $\vec{r_2}$ are vectors that are in the range of [0, 1] and a decreases linearly from 2 to 0 according to the iteration number t.

2) HUNTING

The α, β and δ wolves guide the whole hunting process. The ω wolves update their positions as follows:

$$\vec{X}(t+1) = \frac{\vec{X_1} + \vec{X_2} + \vec{X_3}}{3} \tag{31}$$

where

$$\vec{X_1} = \vec{X_\alpha} - \vec{A_1} \cdot \vec{D_\alpha} \tag{32}$$

$$\vec{X_2} = \vec{X_\beta} - \vec{A_2} \cdot \vec{D_\beta} \tag{33}$$

$$\vec{X_3} = \vec{X_\delta} - \vec{A_3} \cdot \vec{D_\delta} \tag{34}$$

$$\vec{D_\alpha} = \left| \vec{C_1} \cdot \vec{X_\alpha}(t) - \vec{X} \right| \tag{35}$$

$$\vec{D_\beta} = \left| \vec{C_2} \cdot \vec{X_\beta}(t) - \vec{X} \right| \tag{36}$$

$$\vec{D_\delta} = \left| \vec{C_3} \cdot \vec{X_\delta}(t) - \vec{X} \right| \tag{37}$$

3) ATTACKING PREY

When the wolves stop moving, they attack the prey. Using (29), a can implement this process. a is given by

$$a = 2 - \frac{2t}{ter} \tag{38}$$

where ter is the maximum of iterations and t is the iteration number.

4) SEARCH FOR PREY

The search for prey is based on the α, β and δ wolf locations. $\vec{A}$ and $\vec{C}$ control the exploitation and exploration. In the end, the GWO algorithm will stop and output the best position.

The GWO algorithm is demonstrated as follows:

1) Initialize a parent population of *popsize* grey wolves positions;

Initialize a, $\vec{A}$, $\vec{C}$;

2) Based on all wolves' fitness values, the α, β and δ wolves are selected from *popsize* grey wolves.

3) $t = 0$.

while $t \leq ter$ do

For each wolf in the parent population

Update the current wolf's position using (31);

End

Update $\vec{A}$, $\vec{C}$ and a using (29), (30) and (38), respectively;

Evaluate the individual wolves' positions;

Update the α, β and δ positions in the current population;

$t = t + 1$;

End

B. BP NEURAL NETWORK

1) INPUT AND OUTPUT SELECTION

The OP performance is significantly affected by m, N, V and K. Thus, these 17 indicators are used as the input X, and the OP performance is output y. X can be expressed as

$$X = (x_1, x_2, ..., x_{17}) \tag{39}$$

and is used in (16) and (26) to obtain y.

2) NETWORK STRUCTURE

Fig. 2 shows the BP network. For the input layer, there are 17 neurons. For the hidden layer, there are q neurons. For the output layer, there is 1 neuron. For the input and hidden layers, w_{ij} is the weight coefficient, and b_j is the bias. For the hidden and output layers, v_j is the weight coefficient, and θ is the bias. The calculation flow is as follows.

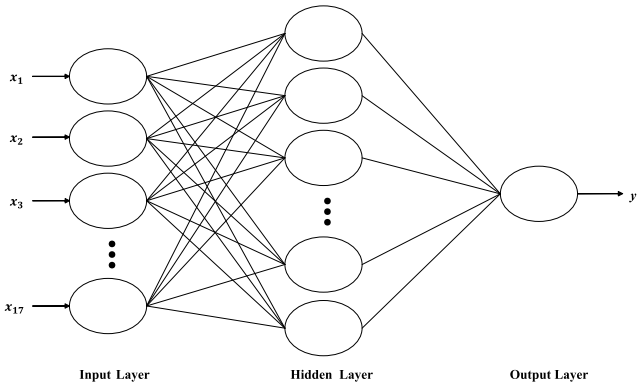

FIGURE 2. The BP neural network structure.

(1) For the hidden layer, the input is

$$s_j = \sum_{i=1}^{17} w_{ij}x_i + b_j, j = 1, 2, ..., q \tag{40}$$

The output is given as

$$c_j = f\left(s_j\right) \tag{41}$$

where f(x) is the activation function.

For the output layer, the input is given as

$$\tau = \sum_{j=1}^{q} v_j c_j + \theta \tag{42}$$

The output is given as

$$y = f\left(\tau\right) \tag{43}$$

(2) y^λ is the output for the λ-th data, and d^λ is the desired output. The overall output error E_r of P training data is given as

$$E_r = \sum_{\lambda=1}^{P} \left(d^\lambda - y^\lambda\right)^2 \tag{44}$$

(3) For different layers, the weights and biases are calculated as follows.

The error of the output layer is given as

$$\delta = (d - y)(1 - y) \tag{45}$$

The error of the hidden layer is given as

$$\sigma_j = \delta v_j (1 - y_j) \tag{46}$$

The weights and biases are then updated as follows

$$v_j = v_j + \eta\delta y_j \tag{47}$$
$$\theta = \theta + \eta\delta \tag{48}$$
$$w_{ij} = w_{ij} + c\sigma_j x_i \tag{49}$$
$$b_j = b_j + c\sigma_j \tag{50}$$

where η is the weight adjustment parameters, $0 < \eta < 1$; and c is learning coefficient, $0 < c < 1$.

C. OP PERFORMANCE PREDICTION BASED ON GWO-BP NEURAL NETWORK

The flowchart of the OP performance prediction algorithm is shown in Fig. 3. The concrete steps are as follows.

(1) The closed form expressions derived previously are used to generate 3050 groups of data and these groups are normalized, 3000 groups are used for training, and the remaining 50 groups are used to test the BP network.

(2) For the BP neural network, small random numbers are used to initialize the bias and weights. The minimum error, maximum number of iterations, and learning rate are also set.

(3) For GWO algorithm initialization, set the number of wolves and the maximum number of iterations. The biases and weights in (40), (42) are used as the initial solution of the GWO algorithm. The GWO algorithm is used to search for the optimal solution.

(4) For BP neural network training, the output of each layer is used to calculate the training error and adjust the bias and weights of the layers. This is repeated until the maximum number of iterations is reached or the error is less than the threshold.

(5) The BP neural network is tested using the test data to determine if the required accuracy is met. If so, the network is used to obtain the OP performance prediction results.

D. METRIC

The mean squared error (MSE) and absolute error (AE) are used to evaluate the performance of the methods. A smaller MSE or AE reflects a higher prediction accuracy. The MSE and AE are given by

$$\text{MSE} = \frac{\sum_{\lambda=1}^{PP} \left(d^\lambda - y^\lambda\right)^2}{PP} \tag{51}$$
$$\text{AE} = \left|d^\lambda - y^\lambda\right| \tag{52}$$

where PP is the number of testing data.

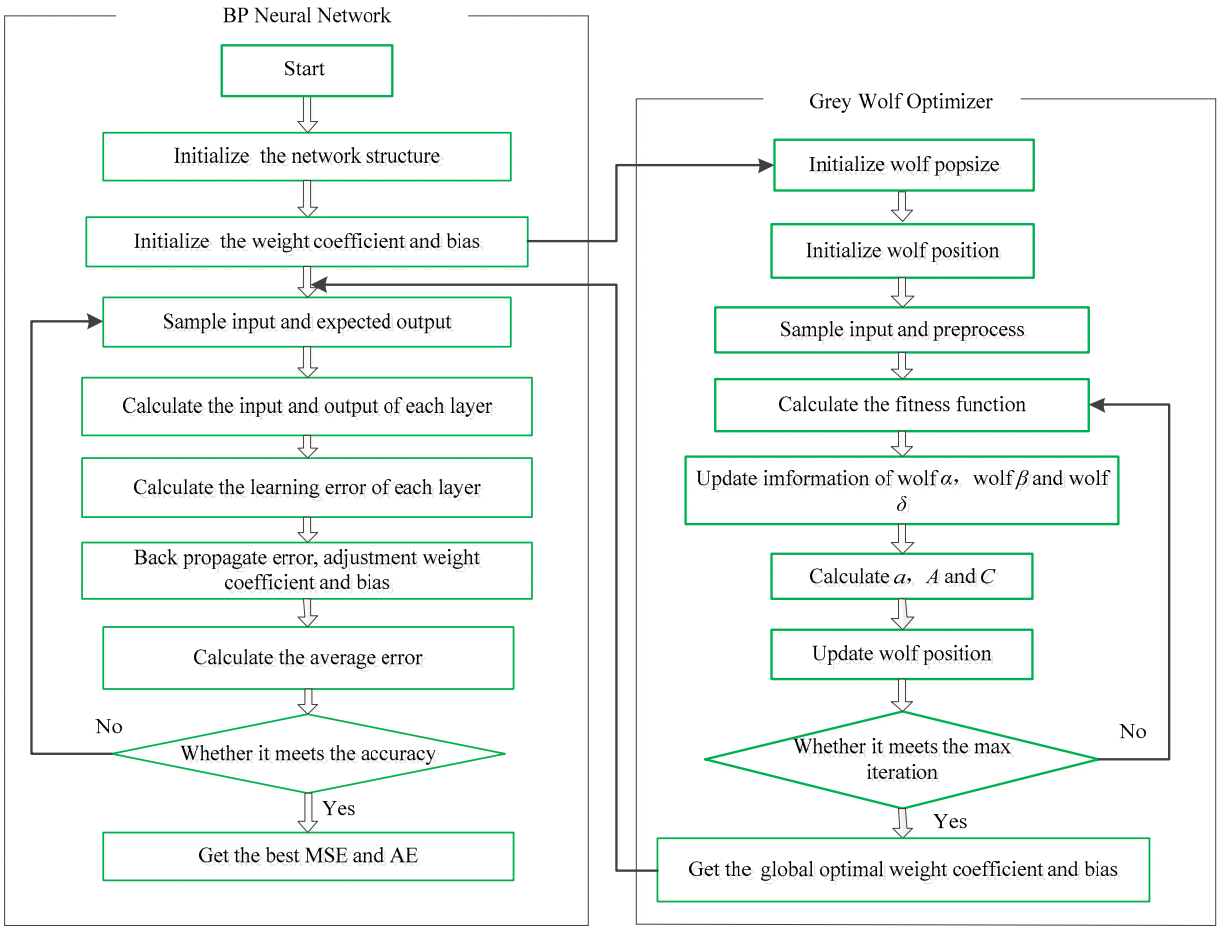

FIGURE 3. The flowchart of the OP performance prediction algorithm.

TABLE 1. Simulation parameters.

Parameters	Values
N_t	1,2,3
L	2
K	0.5
N	2
m	1
μ	0 dB
γ_{th}	5 dB
R_{th}	5 dB

VI. PERFORMANCE RESULTS

Define $\mu=W_{RD}/W_{RE}$ as the relative geometrical gain and let $E=1$.

Table 1 gives the simulation parameters employed for OP performance evaluation. Figs. 4 and 5 present the performance of the TAS I and II schemes, respectively. These figures show close agreement between the analytic and Monte-Carlo simulation results, which validates our analysis. Further, increasing N_t reduces the OP, as expected.

Fig. 6 presents the effect of L on the OP performance with the parameters given in Table 2. This shows that increasing L reduces the OP. For example, for an OP of 1×10^{-3}, increasing L from 2 to 3 improves the performance by more than 2 dB.

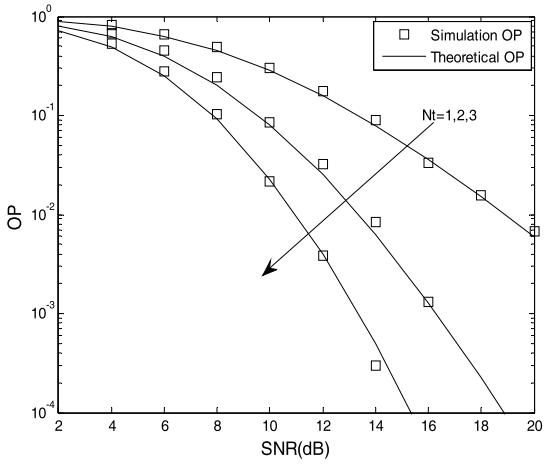

FIGURE 4. The OP performance of TAS I.

Figs. 7 to 18 give the actual and predicted results with the GWO-BP neural network, LWLR [25], SVM [26], ELM [27], wavelet neural network [28] and BP methods. The parameters

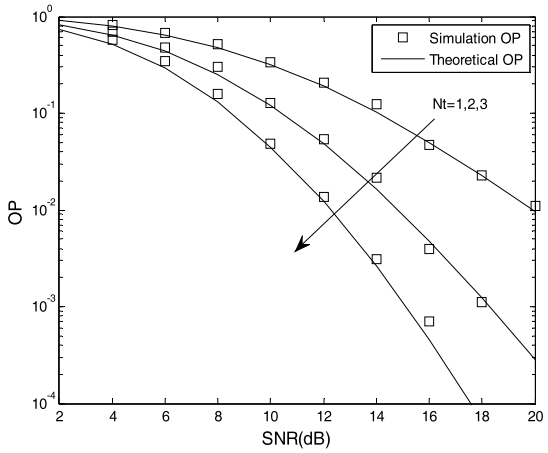

FIGURE 5. The OP performance of TAS II.

TABLE 2. Simulation parameters.

Parameters	Values
N_t	2
L	1, 2, 3
K	0.5
N	2
m	2
μ	0 dB
γ_{th}	5 dB
R_{th}	5 dB

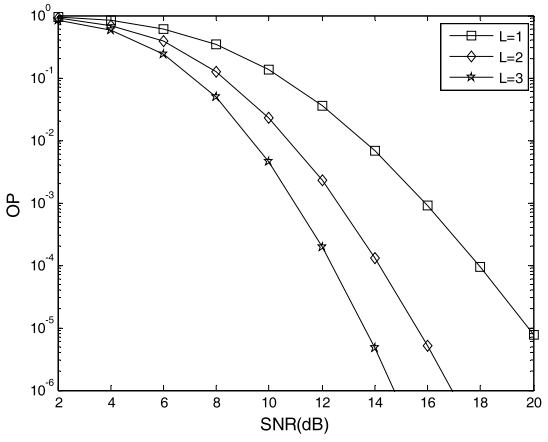

FIGURE 6. The OP performance versus *L*.

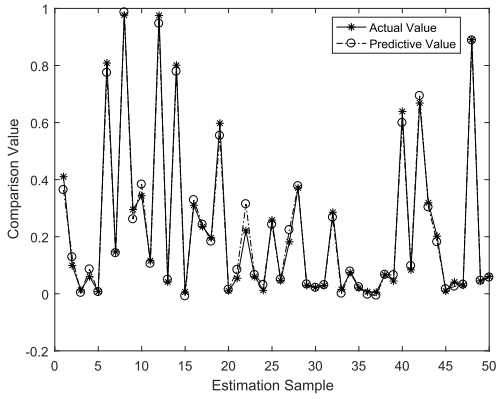

FIGURE 7. Actual and predicted outputs of the GWO-BP neural network.

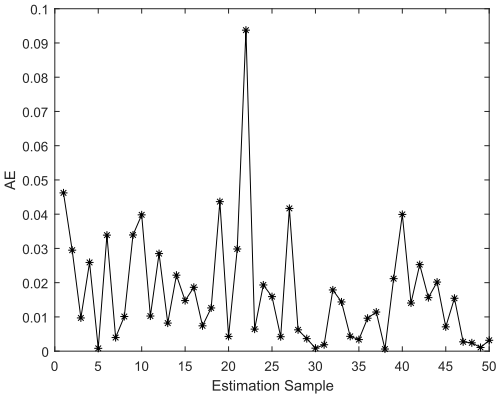

FIGURE 8. AE of the GWO-BP neural network.

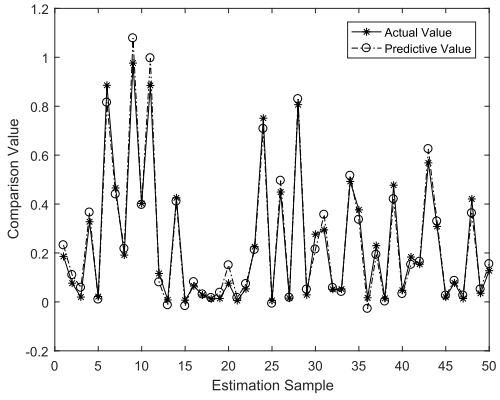

FIGURE 9. Actual and predictive outputs of the BP neural network.

for the six different methods are given in Table 3. From Figures 7-18, we obtain that the MSE of the GWO-BP neural network is 0.000575, and the maximum AE is 0.093742, which are lower than those of the BP, SVM, ELM, wavelet neural network and LWLR methods. Compared to the BP, SVM, ELM, wavelet neural network and LWLR methods, the experimental results verify that the GWO-BP method can consistently achieve higher OP performance prediction result.

Table 4 shows the MSE and AE comparison for six different methods. In Table 4, we obtain that, compared to the ELM, BP, SVR, LWLR, and wavelet neural network methods, the GWO-BP has the smallest MSE and AE. In conclusion, the GWO-BP is the best forecasting model.

Fig. 19 shows the best validation performance. This shows that the MSE generally improves as the number of epochs increases. In our setup, if the validation error increases for

TABLE 3. Simulation parameters.

GWO-BP	BP	ELM	SVM	LWLR	Wavelet Neural Network
X:17 y:1 q:12 Learning rate:0.01 popsize:10 ter:5	X:17 y:1 q:12 Learning rate:0.01	X:17 y:1 q:50000	X:17 y:1 g:0.125 c:1.41	X:17 y:1 Tau:0.8	X:17 y:1 q:13 Learning rate 1:0.01 Learning rate 2:0.001

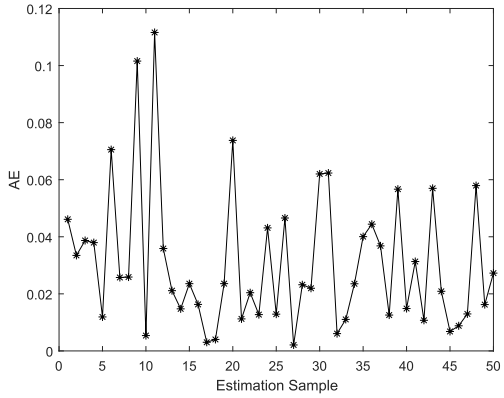

FIGURE 10. AE of the BP neural network.

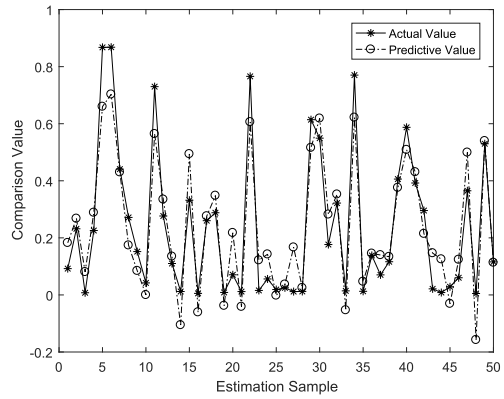

FIGURE 11. Actual and predictive outputs of the SVM.

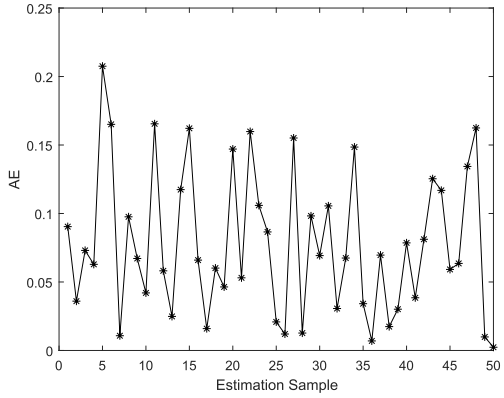

FIGURE 12. AE of the SVM.

20 consecutive steps, the training stops. In Fig. 19, it stops after 92 epochs, while the best validation performance occurs at epoch 72.

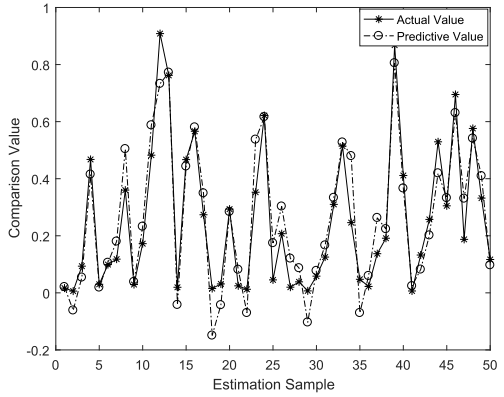

FIGURE 13. Actual and predictive outputs of the ELM.

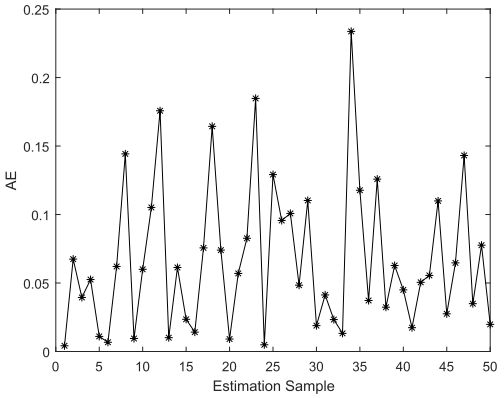

FIGURE 14. AE of the ELM.

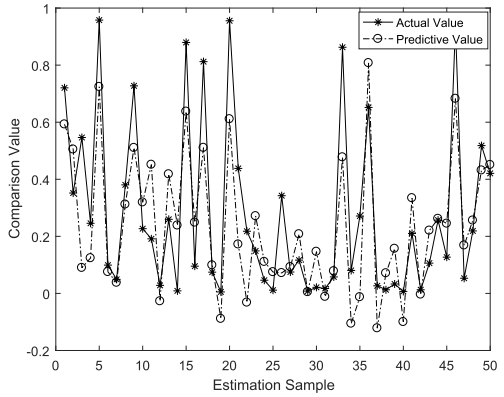

FIGURE 15. Actual and predictive outputs of the wavelet neural network.

In Fig. 20, we can obtain the training state. From Fig. 20, we can see how the gradient changes as the number of iterations increases. After 92 epochs, when the validation checks fail 20 times, the training stage will stop.

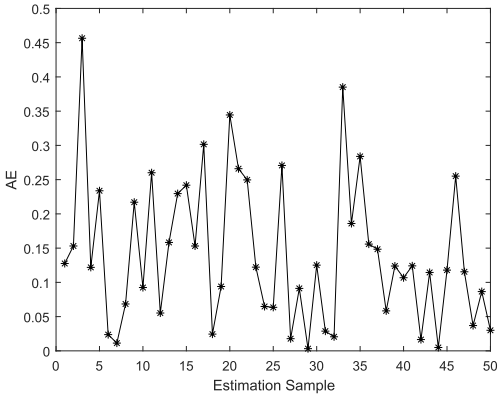

FIGURE 16. AE of the wavelet neural network.

TABLE 4. The AE and MSE comparison of the six methods.

	BP	ELM	SVM	GWO-BP	Wavelet Neural Network	LWLR
AE	0.112	0.234	0.207	0.094	0.456	0.455
MSE	0.002	0.007	0.009	0.001	0.031	0.025

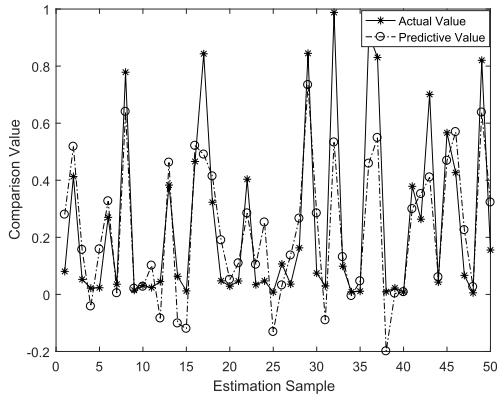

FIGURE 17. Actual and predictive outputs of the LWLR.

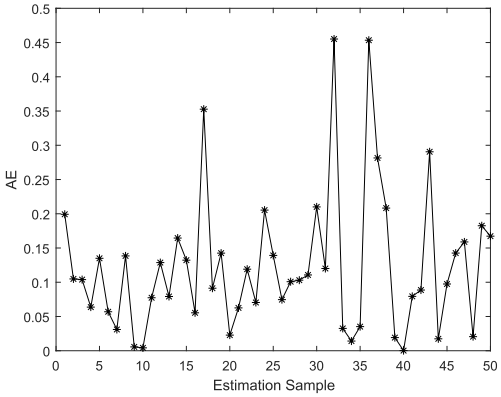

FIGURE 18. AE of the LWLR.

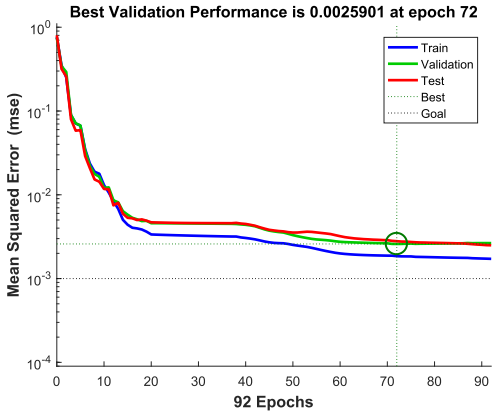

FIGURE 19. The Best validation performance of the GWO-BP neural network.

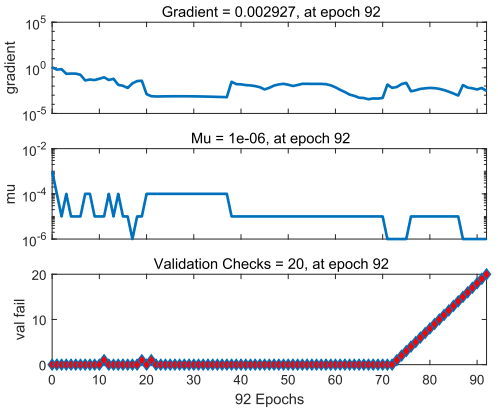

FIGURE 20. The training stage of the GWO-BP neural network.

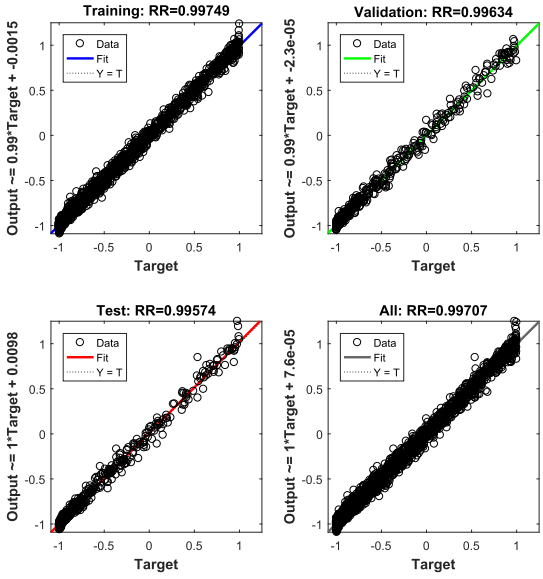

FIGURE 21. The regression of the GWO-BP neural network.

The regression results are shown in Fig. 21. In each plot, the relationship between the targets and outputs is measured by the correlation coefficient *RR*. If *RR* is bigger, the GWO-BP neural network model has a better prediction capability. In Fig. 21, *RR* is 0.99707, which indicates that our method has a good prediction capability.

VII. CONCLUSION

This paper considered OP performance prediction for mobile multiuser communication networks. Closed form expressions were derived for the OP over *N*-Nakagami fading channels. A GWO-BP based OP performance prediction algorithm was proposed. Numerical results were presented which show that this algorithm provides better OP performance prediction results than the wavelet neural network, SVM, LWLR, BP, and ELM methods.

ACKNOWLEDGMENT

The authors would like to thank the editor and the anonymous reviewers for their valuable comments.

REFERENCES

[1] H. J. Huang, S. Guo, G. Gui, Z. Yang, J. H. Zhang, H. Sari, and F. Adachi, "Deep learning for physical-layer 5G wireless techniques: Opportunities, challenges and solutions," *IEEE Wireless Commun.*, to be published. doi: 10.1109/MWC.2019.1900027.

[2] J. L. Sun, W. J. Shi, Z. T. Yang, J. Yang, and G. Gui, "Behavioral modeling and linearization of wideband RF power amplifiers using BiLSTM networks for 5G wireless systems," *IEEE Trans. Veh. Technol.*, to be published. doi: 10.1109/TVT.2019.2925562.

[3] X. Liu, J. Wang, N. Zhao, Y. Chen, S. Zhang, Z. G. Ding, and F. R. Yu, "Placement and power allocation for NOMA-UAV networks," *IEEE Wireless Commun. Lett.*, vol. 8, no. 3, pp. 965–968, Jun. 2019.

[4] N. Zhao, F. Yu, M. Jin, Q. Yan, and V. C. M. Leung, "Interference alignment and its applications: A survey, research issues, and challenges," *IEEE Commun. Surveys Tuts.*, vol. 18, no. 3, pp. 1779–1803, 3rd Quart. 2016.

[5] Y. Cao, N. Zhao, G. Pan, Y. Chen, L. Fan, M. Jin, and M.-S. Alouini, "Secrecy analysis for cooperative NOMA networks with multi-antenna full-duplex relay," *IEEE Trans. Commun.*, vol. 67, no. 8, pp. 5574–5587, Aug. 2019.

[6] G. Gui, H. Sari, and E. Biglieri, "A new definition of fairness for non-orthogonal multiple access," *IEEE Commun. Lett.*, vol. 23, no. 7, pp. 1267–1271, May 2019.

[7] G. Gui, H. Huang, Y. Song, and H. Sari, "Deep learning for an effective nonorthogonal multiple access scheme," *IEEE Trans. Veh. Technol.*, vol. 67, no. 9, pp. 8440–8450, Sep. 2018.

[8] Z. Zhang, W. Shi, Q. Niu, Y. Guo, J. Wang, and H. Luo, "A load-based hybrid MAC protocol for underwater wireless sensor networks," *IEEE Access*, vol. 7, pp. 104542–104552, 2019.

[9] H. Wang, L. Xu, X. Wang, and S. Taheri, "Preamble design with interference cancellation for channel estimation in MIMO-FBMC/OQAM systems," *IEEE Access*, vol. 6, pp. 44072–44081, 2018.

[10] L. W. Xu *et al.*, "Physical layer security performance of mobile vehicular networks," *Mobile Netw. Appl.*, to be published. doi: 10.1007/s11036-019-01224-8.

[11] J. J. Wang, Z. Q. Yan, W. Shi, and X. H. Yang, "Underwater acoustic sparse channel estimation based on DW-SACoSaMP reconstruction algorithm," *IEEE Commun. Lett.*, to be published. doi: 10.1109/LCOMM.2019.2933426.

[12] R. Li, T. Chen, L. Fan, and A. Dang, "Performance analysis of a multiuser dual-hop amplify-and-forward relay system with FSO/RF links," *J. Opt. Commun. Netw.*, vol. 11, no. 7, pp. 362–370, Jul. 2019.

[13] H. Jiang, J. Zhao, L. Shen, H. Cheng, and G. Liu, "Joint integer-forcing precoder design for MIMO multiuser relay system," *IEEE Access*, vol. 7, pp. 81875–81882, 2019.

[14] D. D. Nguyen, V. N. Q. Bao, and Q. Chen, "Secrecy performance of massive MIMO relay-aided downlink with multiuser transmission," *IET Commun.*, vol. 13, no. 9, pp. 1207–1217, Sep. 2019.

[15] Y. Ai, M. Cheffena, A. Mathur, and H. Lei, "On physical layer security of double Rayleigh fading channels for vehicular communications," *IEEE Wireless Commun. Lett.*, vol. 7, no. 6, pp. 1038–1041, Dec. 2018.

[16] A. Pandey and S. Yadav, "Physical layer security in cooperative AF relaying networks with direct links over mixed Rayleigh and double-Rayleigh fading channels," *IEEE Trans. Veh. Technol.*, vol. 67, no. 11, pp. 10615–10630, Nov. 2018.

[17] Y. Alghorani, G. Kaddoum, S. Muhaidat, S. Pierre, and N. Al-Dhahir, "On the performance of multihop-intervehicular communications systems Overn*Rayleigh Fading Channels," *IEEE Wireless Commun. Lett.*, vol. 5, no. 2, pp. 116–119, Apr. 2016.

[18] G. K. Karagiannidis, N. C. Sagias, and P. T. Mathiopoulos, "N*Nakagami: A novel stochastic model for cascaded fading channels," *IEEE Trans. Commun.*, vol. 55, no. 8, pp. 1453–1458, Aug. 2007.

[19] L. Xu, J. Wang, Y. Liu, W. Shi, and T. A. Gulliver, "Outage performance for IDF relaying mobile cooperative networks," *Mobile Netw. Appl.*, vol. 23, no. 6, pp. 1496–1501, Dec. 2018.

[20] L. Xu, J. Wang, H. Zhang, and T. A. Gulliver, "Performance analysis of IAF relaying mobile D2D cooperative networks," *J. Franklin Inst.*, vol. 354, no. 2, pp. 902–916, Jan. 2017.

[21] J. Zhou, H. Qian, X. Lu, Z. Duan, H. Huang, and Z. Shao, "Polynomial activation neural networks: Modeling, stability analysis and coverage BP-training," *Neurocomputing*, vol. 359, no. 24, pp. 227–240, 2019.

[22] B. Jafrasteh and N. Fathianpour, "A hybrid simultaneous perturbation artificial bee colony and back-propagation algorithm for training a local linear radial basis neural network on ore grade estimation," *Neurocomputing*, vol. 235, pp. 217–227, Apr. 2017.

[23] Y. Weng, X. Wang, J. Hua, H. Wang, M. Kang, and F.-Y. Wang, "Forecasting horticultural products price using ARIMA model and neural network based on a large-scale data set collected by Web crawler," *IEEE Trans. Comput. Social Syst.*, vol. 6, no. 3, pp. 547–553, Jun. 2019.

[24] E. Emary, H. M. Zawbaa, and C. Grosan, "Experienced gray wolf optimization through reinforcement learning and neural networks," *IEEE Trans. Neural Netw. Learn. Syst.*, vol. 29, no. 3, pp. 681–694, Mar. 2018.

[25] T. De Cola and M. Mongelli, "Adaptive time window linear regression for outage prediction in Q/V band satellite systems," *IEEE Wireless Commun. Lett.*, vol. 7, no. 5, pp. 808–811, Oct. 2018.

[26] X. Li, X. Jia, L. Wang, and K. Zhao, "On spectral unmixing resolution using extended support vector machines," *IEEE Trans. Geosci. Remote Sens.*, vol. 53, no. 9, pp. 4985–4996, Sep. 2015.

[27] K.-K. Xu, H.-D. Yang, and C.-J. Zhu, "A novel extreme learning Machine-based Hammerstein-Wiener model for complex nonlinear industrial processes," *Neurocomputing*, vol. 358, pp. 246–254, Sep. 2019.

[28] X. Shen, F. Zhang, H. Lv, J. Liu, and H. Liu, "Prediction of entering percentage into expressway service areas based on wavelet neural networks and genetic algorithms," *IEEE Access*, vol. 7, pp. 54562–54574, 2019.

LINGWEI XU was born in Shandong, China, in 1987. He received the B.S. degree from the Department of Communication and Electronics, Qingdao Technological University, Qingdao, China, in 2011, the M.S. degree in electronic and communication engineering and the Ph.D. degree in intelligent information and communication system from the Ocean University of China, Qingdao, in 2013 and 2016, respectively. Since 2016, he has been an Associate Professor with the College of Information Science and Technology, Qingdao University of Science and Technology. He has published about 60 research articles in international SCI/EI journals and conferences. His research interests include UWB systems, MIMO wireless systems and networking, cooperative communications and networking, M2M communications and networking, D2D communications, and 5G mobile wireless communications.

HAN WANG received the B.S. degree in electrical engineering from the Hubei University of Nationalities, China, in 2009, and the M.S. and Ph.D. degrees in information and communication system from Hainan University, Haikou, China, in 2013 and 2017, respectively. He has worked in China Mobile Jiangxi Branch as a Network Engineer for one year. He is currently an Associate Professor with Yichun University. His research interests include wireless sensor networks, filter-bank multicarrier communications, and information theory.

WEN LIN received the Ph.D. degree in communication and information engineering from the Xiamen University, China, in 2012. Since 2012, he has been an Associate Professor with the College of Computer and Control Engineering, Minjiang University. He is mainly involved in the research of underwater acoustic network communication, wireless network protocol, and network chromatography.

THOMAS AARON GULLIVER (SM'96) received the Ph.D. degree in electrical engineering from the University of Victoria, Victoria, BC, Canada, in 1989. From 1989 to 1991, he was a Defence Scientist with the Defence Research Establishment Ottawa, Ottawa, ON, Canada. He has held academic positions at Carleton University, Ottawa, and the University of Canterbury, Christchurch, New Zealand. He joined the University of Victoria, in 1999, and is currently a Professor with the Department of Electrical and Computer Engineering. His research interests include information theory and communication theory, algebraic coding theory, cryptography, multicarrier systems, smart grid, intelligent networks, cryptography, and security. In 2002, he became a Fellow of the Engineering Institute of Canada and a Fellow of the Canadian Academy of Engineering, in 2012.

KHOA N. LE received the Ph.D. degree from Monash University, Melbourne, Australia, in October 2002. From April 2003 to June 2009, he was a Lecturer with Griffith University, Gold Coast campus, Griffith School of Engineering. From January to July 2008, he was a Visiting Professor with the Intelligence Signal Processing Laboratory, Korea University, Seoul, South Korea. From January 2009 to February 2009, he was a Visiting Professor with the Wireless Communication Centre, University Technology Malaysia, Johor Bahru, Malaysia. He is currently an Associate Professor with the School of Computing, Engineering, and Mathematics, Western Sydney University, Kingswood. His research interests include in wireless communications with applications to structural and construction management problems, image processing, and wavelet theory. Since 2003, he has been an Editor of the *Journal on Computer Networks and Communications*. He was a Guest Editor of a special issue of Physical Communication, in 2012, on Polarization in Wireless Communications. Since 2018, he has been an Editor for the IEEE TRANSACTIONS ON VEHICULAR TECHNOLOGY and *IET Signal Processing*.